

Original Research

Spatial and Temporal Distribution Characteristics of Rainstorm and Flood Disasters Around Tarim Basin

Baoxin Chen¹, Kan Chen¹, Xi Wang^{1*}, Xu Wang^{2}**

¹School of Humanities and Social Sciences, Macao Polytechnic Institute, Macao, 999078, PR China

²Xinjiang Uygur Autonomous Region Weather Modification Office, Urumqi, 830002, PR China

Received: 2 September 2021

Accepted: 4 November 2021

Abstract

The Tarim Basin is highly vulnerable to rainstorm and flood disasters, related to its special position of C-shaped terrain in the westerly belt and the ever-present monsoons. According to data of the storms and floods that occurred near the Tarim Basin from 1980 to 2019, the proportional weight method was used to construct the disaster exponent; whereas, the percentile method was used for classification. As a result, the disaster level is divided into four grades: mild, moderate, severe, and extremely severe. The results also indicated a phenomenon: the geographical frequency distribution of rainstorm and flood disasters around the basin shows more occurrences in the west and north, and less in the east and south, and occur mainly from April to September (in spring and summer); and June and July are the high incidence periods. The annual frequency of rainstorm and flood disasters around the basin showed a significant linear growth trend from 1980 to 2019, that is, an increase of 8.6 times every 10 years. However, the annual disaster exponent changed abruptly in 1985 and 1999, when the average values of the disaster exponent in 1980-1985, 1986-1999 and 2000-2019 were 7.63, 64.66 and 25.80, respectively. The contribution rates of annual occurrence times of disasters with Grades 1 to 4 to damage exponent are 4%, 2%, 24% and 70%. In conclusion, to better mitigate rainstorm and flood disasters in the basin, focus of optimal prevention should occur Grade 3 and Grade 4 rainstorm and flood disasters.

Keywords: Tarim Basin, rainstorm and flood, disaster exponent, grade division, spatial and temporal distribution

*e-mail: xwang@ipm.edu.mo

**e-mail: wangxu2323@vip.163.com

Introduction

The term “rainstorm and flood disaster” refers to flood and waterlogging meteorological disasters that are easily affected by multiple factors, such as, rainfall intensity, topography, and underlying surface geology [1-3]. These types of disasters become some of the costliest natural disasters globally, especially in remote and impoverished areas; these often lead to massive life and property losses (the loss of 1.94 million lives and economic losses of US\$ 2.4 trillion From 1970 to 2012) [4-5]. Although the surrounding area of Tarim Basin is a typical arid area, rainstorm events occur every year [6]. Since the 1980s, climate has become humid and warm, the precipitation around the Tarim Basin increased, and the short-term heavy rainfall increased significantly [7], resulting in a bulge in rainstorm and flood disasters. The disaster risk analysis, in line with the natural disaster risk theory, is carried out thus, using these four items: the risk of disaster-causing factors, the sensitivity of disaster-pregnant environment, the vulnerability of disaster-affected bodies and the ability of disaster prevention and mitigation [8].

Disaster risk assessment uses gathered research on meteorological disaster risk zoning and is utilized in this manner: as an index evaluation, a probability distribution of disaster factors, and a scenario simulation evaluation [9]. Not only so, risk research methods are also moving towards quantitative research, not just risk qualitative description [10]; with the progress of analytical technology, many improved and combined methods for quantitative assessment are becoming valuable assets to tap into: For example, Orton et al. [11] applied a three-dimensional hydrodynamic model in flood hazard assessment; Dyer [12] demonstrated the applicability of the AHP optimization model; Liu J. et al. [13] used the Delphi method to determine the weight of the disaster factor; Xiao W. et al. [14] integrated the index of entropy and linear weighted analysis to classify the disaster situation; Xiao Y. et al. [15] incorporated spatial ordered weighted averaging method into a windows-based local spatial multi-criteria analysis; Yang et al. [16] integrated a fuzzy comprehensive evaluation method with a coordinated development degree model and Liu R. et al. [17] coupled weighted naïve Bayes, geographic information system (GIS), and remote sensing; Metternicht et al. [18] developed a web-based database/GIS structure; Balogun et al. [19] proposed an integrated GIS fuzzy multi-criteria decision making model; Rahman et al. [20] used machine learning algorithm to consider the dynamic nature and spatial aspects of predicting potential flood events. These additional scientific assessment tools can help to mitigate the risk of rainstorm and flood disaster in order to simulate, deduce, evaluate and predict by the establishment of a mathematical model [21-22]. Further, the grade divisions of disaster, are determined by dividing the threshold interval of disaster factors subjectively;

and the spatial distribution characteristics of different grades of disasters are carried out [23-26].

The combination of geographic information system technology, data visualization and disaster assessment methods have become a popular trend. This article uses ratio weights and dimensionless linear summing, as well as calculating the disaster loss index and grading to further implement the visualization of the disaster severity, which has not been studied. It is also, collectively the use of flood disaster data in a typical arid area or semi-arid during these past 40 years. However, previous studies have not studied rainstorm and flood disasters around the Tarim Basin. The temporal and spatial distribution characteristics of rainstorm and flood disasters around the basin are presently, in this study, being analyzed according to the disaster exponent and grade division. The purpose is to provide a solid basis for scientific disaster prevention and mitigation, as well to standardize and provide a classic way of thinking about the law of flood disasters.

Experimental

Overview of the Study Area

The Tarim Basin is surrounded by the Tianshan Mountains, the Kunlun Mountains and the Altun Mountains; it is situated east of the Pamir Plateau and is the largest inland basin in the world (Fig. 1). The special C-shaped terrain compounds the weather complications by its position in the westerly belt and the ever-present monsoons [27-28]. Although the annual precipitation volume around the basin is much lower than the domestic average, there are many rainstorms and short-term heavy rainfalls, often cause rainstorms and floods. To facilitate the systematic study to compare and analyze the rainstorm and flood disasters around the basin, the surrounding areas of the basin are divided into four parts: the eastern, the western, the southern and the northern. The Bayingoleng Mongolian Autonomous Prefecture (Bazhou) belongs to the eastern part of the basin, and the Kizilsu Kirgiz Autonomous Prefecture (Kezhou) and Kashgar Prefecture are located in the western part of the basin. The Hotan Prefecture and Aksu Prefecture, respectively, refer to the southern and northern parts of the basin.

Data

This paper is based on the rainstorm and flood disaster information recorded by the Civil Affairs Department of Xinjiang Uygur Autonomous Region; it sorts out 42 counties and cities around the Tarim Basin during 1980-2019 and includes 1) the occurrence time (year and month), 2) the occurrence area (counties and cities), 3) and the number of deaths (persons); also, 4) the number of collapsed homes (houses),

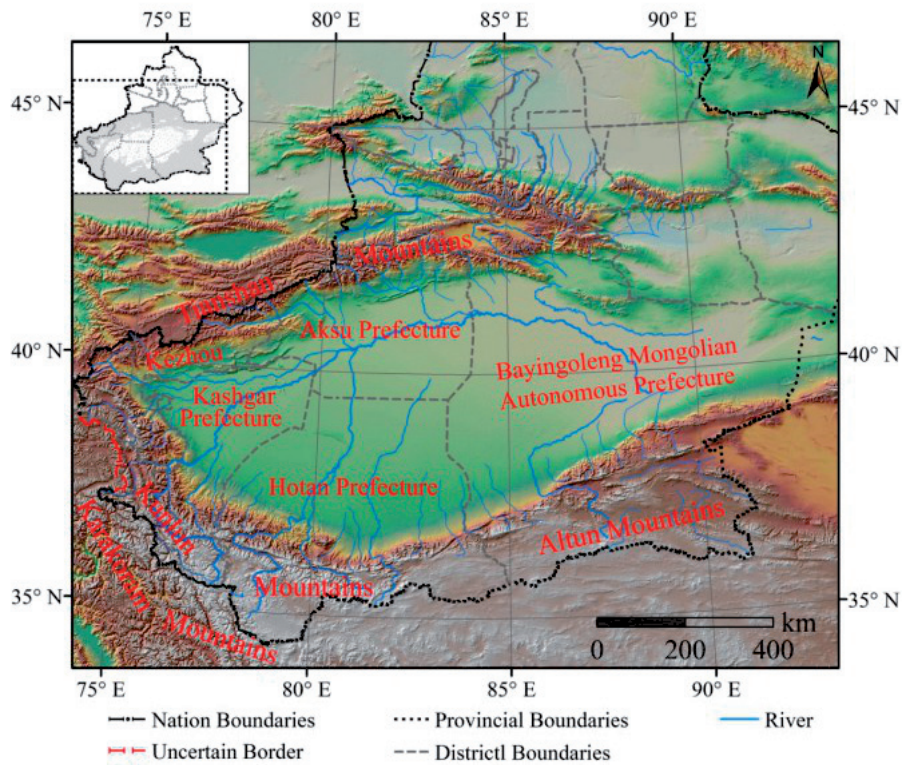


Fig. 1. Topography and administrative map of Tarim Basin.

5) the number of collapsed sheds (seats), 6) the number of livestock deaths (heads), and 7) the affected area of crops (hm²). If there is a rainstorm and flood disaster in a county, the number of rainstorm and flood disasters in the county is recorded as 1.

Methods

There are five disaster factors expressing a rainstorm and flood disaster event; in order to compare the strength of different disaster events, a disaster exponent (Z_i) which can comprehensively express the five disaster factors is constructed. Thus, in the construction of Z_i , the weight of a single disaster factor is first determined by the ratio method; then Z_i is obtained by a dimensionless linear summation method. Assuming that there are m disaster factors, and each factor is composed of n samples, the disaster factor evaluation matrix ($X_{n \times m}$) can be obtained. The calculation formula is defined as follows:

$$Z_i = \sum_{j=1}^m \frac{\sum_{i=1}^n \frac{X_{ij}}{X_{Maxj}}}{\sum_{j=1}^m \sum_{i=1}^n \frac{X_{ij}}{X_{Maxj}}} \frac{X_{ij}}{\bar{X}_j} \tag{1}$$

In this formula, $i = 1, 2, \dots, n$, n represents the total number of disaster events ($n = 1467$). $j = 1, 2, \dots, m$, and m represents disaster factors ($m = 5$). \bar{X}_j , X_{Maxj} represents the average and maximum of the j -th disaster

element respectively. The weight of the first disaster factor is expressed as:

$$\frac{\sum_{i=1}^n \frac{X_{ij}}{X_{Maxj}}}{\sum_{j=1}^m \sum_{i=1}^n \frac{X_{ij}}{X_{Maxj}}} \tag{2}$$

After the calculation of formula (1), the weight coefficient, the average and the maximum value of five disaster factors can be noted in Table 1.

The percentile method is used to determine the damage exponent grade [29]. Percentile is a kind of position exponent. According to the range of threshold change, the disaster is divided into four grades (specific results are listed in Table 2).

Results

Spatial Distribution of Rainstorm and Flood Disaster

Significant differences in the frequency of rainstorm and flood disasters occurred in 42 counties around the Tarim Basin from 1980 to 2019. For example, the mean occurrence times of disaster and in specified counties and cities can be noted: eastern (23), western (36), southern (30), and northern (50) regions of the basin. Disasters occur more frequently in the west and north of the basin, and less in the east and south. Among them, the rainstorm and flood disasters occurred

Table 1. Weight coefficient, average and maximum value of disaster factors.

	Deaths (persons)	Collapsed homes (houses)	Collapsed sheds (seats)	Livestock deaths (heads)	Crops affected area (hm ²)
Weight coefficient	0.12	0.35	0.06	0.25	0.22
Average value	0.4	153.4	78.0	518.1	1488.4
Maximum value	35	4354	12000	20366	66530

Table 2. Grading criteria of rainstorm and flood disasters around Tarim Basin.

Percentile r (%)	Disaster exponent Z_i	Disaster grade
$r \leq 50$	$Z_i \leq 0.33049$	Mild (Grade 1)
$50.1 \leq r \leq 75$	$0.33050 \leq r \leq 1.13040$	Moderate (Grade 2)
$75.1 \leq r \leq 90$	$1.13041 \leq r \leq 2.69718$	Severe (Grade 3)
$r \geq 90.1$	$Z_i \geq 2.69719$	Extremely severe (Grade 4)

most often in Baicheng County, with an average of 2.2 times per year, followed by Wensu County, with an average of 1.8 times per year (Fig. 2a). Viewing the spatial distribution map of the annual average disaster exponent (Fig. 2b), a clear pattern from the perspective of the counties and cities emerges: the ranking order of annual average disaster exponent from large to small is: the north (1.33), the west (0.98), the south (0.55) and the east (0.51). Thus, in general, the flood disasters around the basin are strong in the northwest and weak in the southeast. As a result, areas with a high frequency of disasters and a high damage exponent appear in the Aksu area (on the south side of Tianshan Mountains) and Kashi area (in the western part of Southern Xinjiang). Interestingly, several counties with heavy rainstorm and flood disasters in these two areas are often contiguous. Further, one can note the geographical distribution of disasters is similar to the spatial distribution of rainstorm frequency around the basin.

Considering, strictly from the statistical side, the rainstorm and flood disasters, the occurrence times of Grades 1-4 were 733, 367, 220 and 147, respectively. The occurrence times of different grades, from 1 to 4, around the basin were in this order: north, west, south and east (Fig. 3). Among them, 1) Baicheng County had the highest occurrence of Grade 1 disasters (an average of 1.6 times per year); 2) Kuche County had the highest Grade 2 disasters (an average of 0.5 times per year); 3) Yecheng County had the highest Grade 3 disasters (an average of 0.3 times per year); and 4) Aksu City had the highest Grade 4 disasters (an average of 0.3 times per year).

Seasonal and Monthly Distribution of Rainstorm and Flood Disaster

The majority of rainstorm and flood disasters around the Tarim Basin occur mainly in spring and summer, specifically, from April to September, and accounts

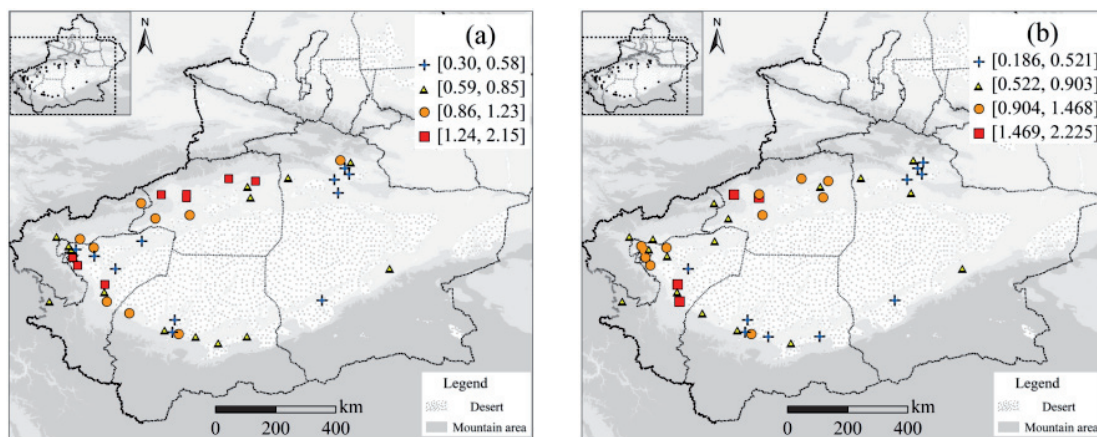


Fig. 2. Spatial distribution of annual average occurrence frequency and annual average disaster exponent of rainstorm and flood disasters around the basin. a) average annual occurrences (times), b) average annual damage exponent.

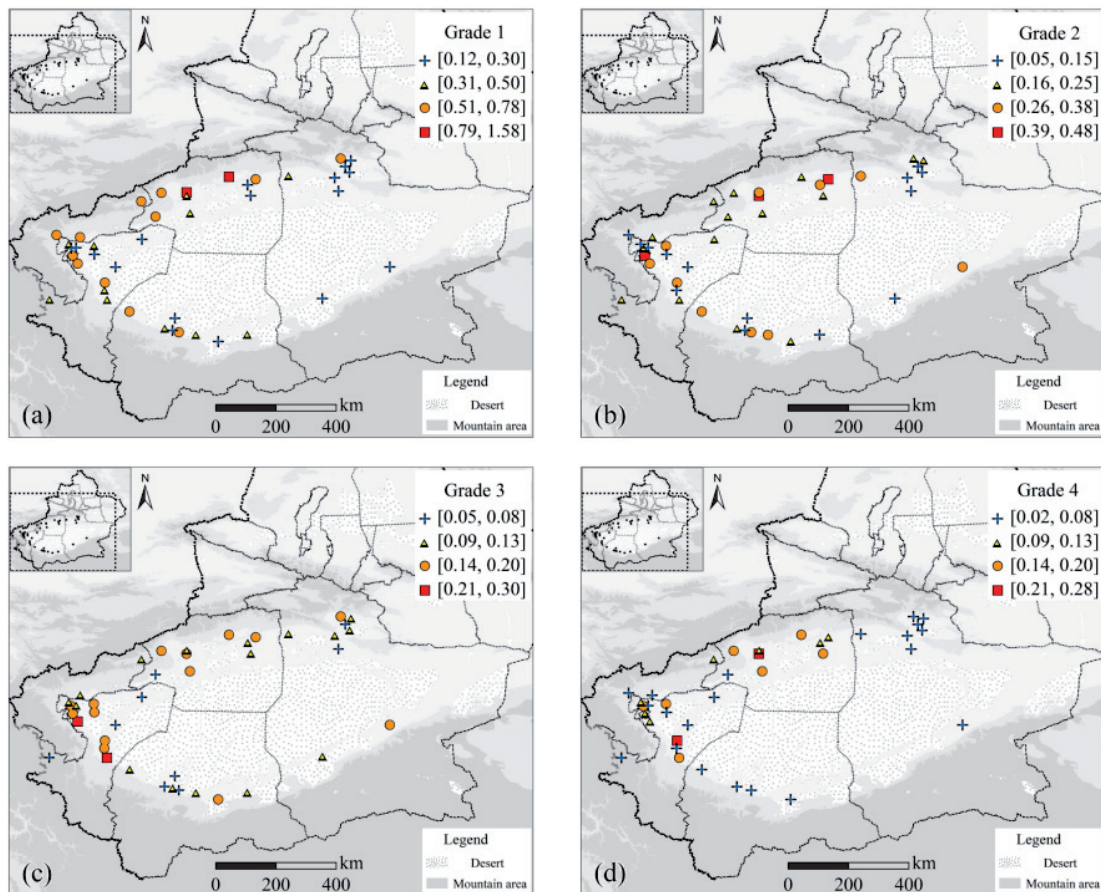


Fig. 3. Spatial distribution of average annual occurrence frequency of Grades1-4 rainstorm and flood disasters around the basin

for 97% of the yearly total. Yet, the highest, most intense period of rainstorm and flood disasters occur in the June-July time frame (summer), yet still accounts for 56% of the yearly total. In addition, rainstorm and flood disasters of Grades 1- 4 around the basin show a unimodal distribution (Fig. 4). Among them, Grade 1 disasters appear most frequently in July, 31% of the annual occurrence frequency; Grade 2 disasters appear most frequently in June, 35% of the whole year; Grade 3 disasters also appear most frequently in June, 31% of the whole year, and finally, Grade 4 disasters appear most frequently in July, 29% of the year.

Interannual Variation of Rainstorm and Flood Disaster

Around the Tarim Basin, during 1980-2019, the annual frequency of rainstorm and flood disasters showed a significant linear growth trend, increasing 8.6 times every 10 years (Fig. 5a). However, there is no linear increase or decrease in the annual disaster exponent, but, rather, a ladder-like change, weak at both ends and strong in the middle (Fig. 5b). In addition, unexpectedly, the cumulative departure curve test showed that the annual disaster exponent had mutations

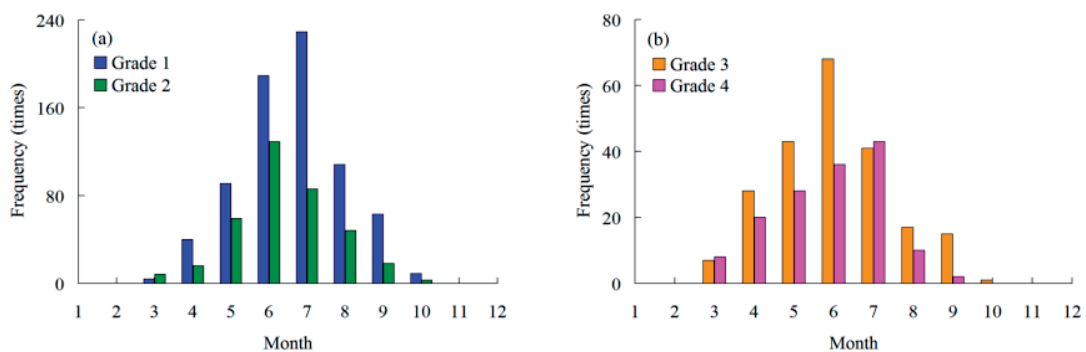


Fig. 4. Seasonal variation of occurrence frequency of rainstorm and flood disasters around the basin.

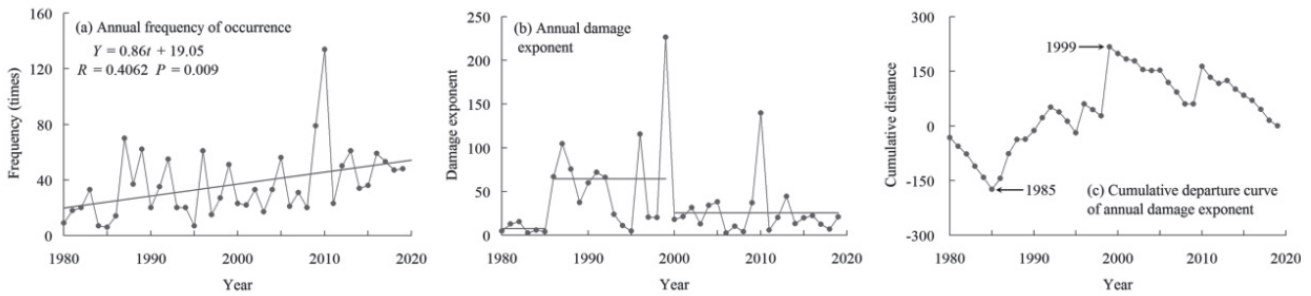


Fig. 5. Annual frequency of rainstorm and flood disasters around the basin, interannual variation of annual disaster exponent and mutation test of annual disaster exponent, average grade line in figure b). R indicates the correlation coefficient, P indicates the level of reliability. The straight line indicates a linear trend in figure a).

in 1985 and 1999 (Fig. 5c). Further, 1980-1985, 1986-1999 and 2000-2019 showed, the average annual disaster exponent fluctuated, 7.63, 64.66 and 25.80, respectively. It was observed that, from the late 1980s to the end of the 20-th century, basin disasters were the strongest, and the disaster intensity was 2.5 times of the first 20 years of the 21-st century.

Fig. 6 shows the inter-annual variation of the number of occurrences of Grades 1-4 rainstorm and flood disasters. The number of occurrences of Grade 1 disasters fluctuated around 10.3 times of the annual average from 1980 to 1990, showing a significant linear growth trend from 1991 to 2019, increasing by 15.1 times every 10 years. The annual frequency of Grades 2-4 disasters fluctuated around the average climate. Among them, Grade 2 disasters had

maximum values in 1989, 1992, 1996 and 2010, and their maximum values were more than 25 times. The number of occurrences of Grade 3 disasters reached the maximum in 2010, reaching 34 times. The maximum number of Grade 4 disasters occurred in 1999, up to 32 times.

The contribution rate of annual occurrences of rainstorm and flood disasters with Grades 1- 4 to annual disaster exponent can be described by the coefficients of multiple linear regression equations between annual occurrences and annual disaster exponent. This assumes the standardized sample sequences of the number of occurrences in Grades 1 to 4 and the annual disaster exponent are y_1, y_2, y_3, y_4 and z_y , respectively, the multiple regression equation is $z_y = 0.048 y_1 + 0.024 y_2 + 0.284 y_3 + 0.833 y_4$ ($R = 0.9764, P = 8.7 \times 10^{-23}$).

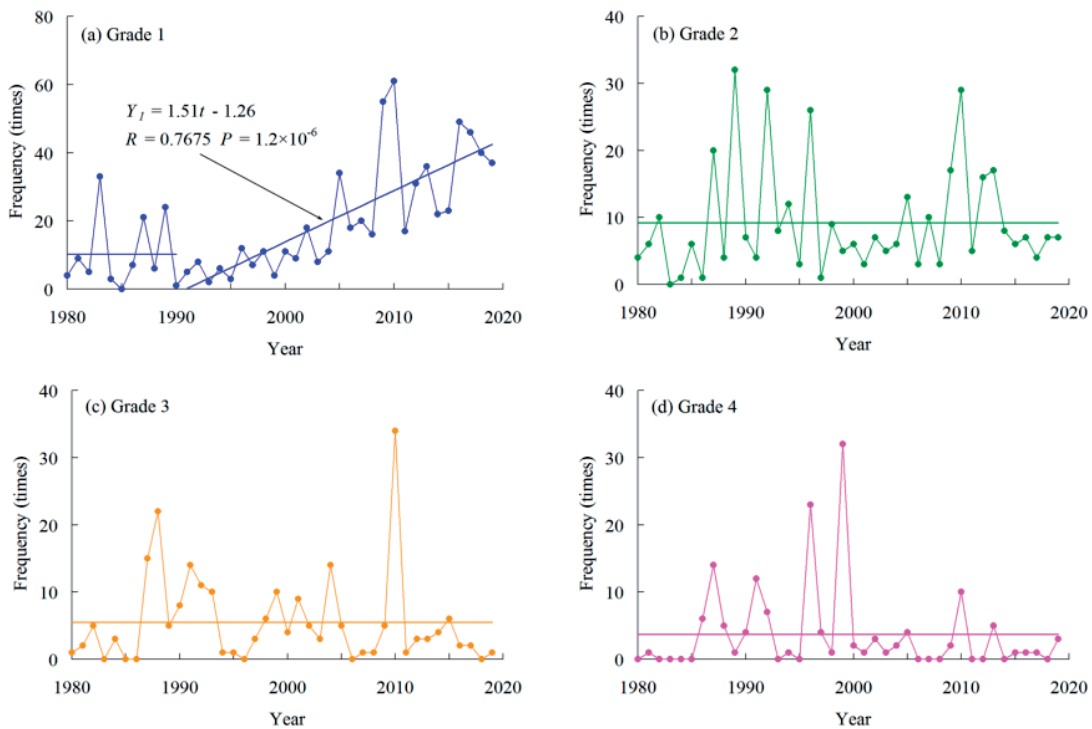


Fig. 6. Interannual variations in the number of occurrences of rainstorms and floods of Grades 1-4 around the basin, with the average grade line in the figure.

The regression equation is significant and the coefficients of the equation are positive: this, indicates that the annual disaster exponent increases with the increase in the number of occurrences. Thus, the percentage of a single regression coefficient in the total value of the four coefficients stands for the contribution rate of the number of disasters at different Grades to the annual disaster exponent. The annual number of disasters from Grade 1 to Grade 4 contributed 4%, 2%, 24% and 70% to the annual damage exponent, respectively. It can be observed that the contribution rate of Grade 4 disasters is the highest, followed by Grade 3. This further shows that although the Grade 1 disasters show a significant linear growth trend after 1991, both the Grade 4 and Grade 3 disasters do not show a linear growth trend, so the annual disaster exponent will not show a linear growth trend. In addition, the occurrence times of Grade 3 and Grade 4 disasters in the disaster years (1986-1999) was relatively high, resulting in the peak average annual disaster exponent at this stage. Finally, the occurrence of Grade 3 and Grade 4 disasters should be focused on in a directed and intensive basin rainstorm and flood disaster prevention program.

Discussion

From the perspective of spatial distribution, rainstorm and flood disasters shows more occurrences (stronger) in the west and north Tarim Basin, and less (weaker) in the east and south. Baicheng County and Wensu County have the highest and second highest annual average disaster occurrences, respectively. But the disaster grade in Aksu City and Shache County was the strongest and the second highest, respectively. Grades 1-4 disasters occurred more frequently in northwest basin and less in southeast basin.

It is worth noting that "the principle" of flood disasters in the Siberian Basin, the largest area in the world, is the same as that in the Tarim Basin. However, unlike the distribution of flood disasters in the Tarim Basin in this study, the southern part of the Siberian Basin is dominated by III & IV-level floods, and the central part is the most densely populated. In the region, flooding is the most harmful, and the lowest flood risk is in the north. It is mainly the I-level flood and rarely at the II-level flood [30].

The rainstorm and flood disasters around the Siberian basin mainly emerged from April to September, accounting for 97% of the year, and concentrated in June and July, accounting for 56% of the year. Grade 1 and Grade 4 disasters occurred most frequently in July, when Grade 2 and Grade 3 disasters occurred mostly in June. Kichigina [30] analyzed the occurrence pattern of the Siberian Basin from 1985 to 2016. The floods in Siberia most frequently occurred during snowmelt (18% of floods) and summer rainfall (44% of floods). For the monthly inundation extent, Papa et

al. [31] pointed out that the river's ice, which usually freezes at the beginning of October, thaws at the end of April or the beginning of May of the following year. The temperature in western Siberia is warmer in the winter and spring, and the snowmelt season in this area starts around April and gradually advances eastward.

Conversely, most of the floods on the west coast of the United States are caused by Pacific, tropical cyclones that reach the west coast mountains, a regular, seasonal phenomena. Those flash floods start to increase in November and reach the highest frequency in December, and basically ending this season in April [32]. Most of the floods in the eastern United States come from tropical cyclones in the North Atlantic, which are more common in the autumn. We saw a relatively largest flash flood which was observed in September [33].

The classification of flood hazards vary both within and across topography, flood type, duration, and source of flash floods. Presently, no unified classification standard exists. This study innovatively correlates the number of occurrences of rainstorms and flood disasters of grades 1-4 to contribution rate of the annual disaster index. The occurrence times of Grade 1 disasters in 1991-2019 showed a significant linear growth trend, increasing by 15.1 times every 10 years. In the past 40 years, the number of disasters of Grades 2-4 fluctuated around the average times. The contribution rates of annual disaster occurrences with Grades 1-4 to annual damage index were 4%, 2%, 24% and 70%, respectively.

Conclusions

As was previously noted in this study, the rainstorm and flood disasters around the basin mainly emerged from April to September, accounting for 97% of the year, and concentrated in June and July, accounting for 56% of the year. Grade 1 and Grade 4 disasters occurred most frequently in July, when Grade 2 and Grade 3 disasters occurred mostly in June. The frequent occurrence of rainstorm and flood disasters in the basin and the heavy disaster areas are distributed in the Aksu area and Kashgar area. It is necessary, therefore, to strengthen the prediction, early warning, and defense of rainstorm and flood disasters in these areas during disaster-prone period.

It appears, through the use of statistical data, that the annual frequency of rainstorm and flood disasters around Tarim basin showed a significant linear growth trend from 1980 to 2019, with an increase of 8.6 times per 10 years. The annual disaster exponent showed a ladder-like change with weak at both ends and strong at the middle, and mutation occurred both in 1985 and 1999. The average annual disaster exponent in 1980-1985, 1986-1999 and 2000-2019 were 7.63, 64.66 and 25.80, respectively. Further, the contribution rate of disasters with Grade 4 is the highest, followed by Grade 3.

Therefore, the prevention of rainstorm and flood disasters in Tarim Basin, the occurrence of Grade 3 and Grade 4 disasters should be of the utmost focus; applying rigorous and scientific measures can help mitigate these meteorological events from continually having severe and potentially disastrous effects on the area and its population.

Finally, according to temporal and spatial distribution characteristics of local disasters, disaster prevention and mitigation arrangements have been made. There are many methods for evaluating the severity of disasters; however, these methods have many indicators, heavy calculation workloads, and rely on advanced technology and equipment; also, these measures have low universality and a small application range. The five disaster loss indicators used in this article are representative, and the data statistical methods used are universally applicable, providing a certain reference value for the classification of the degree of natural disasters in various places.

Acknowledgments

This work was supported by Foundation of Xinjiang weather modification (RYB202002). Thanks are due to Mr. Michael J. Manzullo, (Adjunct English Professor, Baylor University) for English improvement of this article.

Conflict of Interest

The authors declare no conflict of interest.

References

- GUO J., WU X., WEI G. A new economic loss assessment system for urban severe rainfall and flooding disasters based on big data fusion. *Environmental research*. **188**, 109822, **2020**.
- MEHRYAR S., SURMINSKI S. National laws for enhancing flood resilience in the context of climate change: potential and shortcomings. *Climate Policy*. **21** (2), 133, **2021**.
- MANDEL A., TIGGELOVEN T., LINCKE D., KOKS E., WARD P., HINKEL J. Risks on global financial stability induced by climate change: the case of flood risks. *Climatic Change*. **166** (1), 4, **2021**.
- World Meteorological Organization (WMO). Atlas of mortality and economic losses from weather, climate and water extremes (1970-2012). available at <https://library.wmo.int/doc_num.php?explnum_id=7839>
- ADNAN M.S.G., ABDULLAH A.Y.M., DEWAN A., HALL J.W. The effects of changing land use and flood hazard on poverty in coastal Bangladesh. *Land Use Policy*. **99**, 104868, **2020**.
- ZHOU Y.S., XIE Z.M., LIU X. An analysis of moisture sources of torrential rainfall events over Xinjiang, China. *Journal of Hydrometeorology*. **20** (10), 2109, **2019**.
- ZHANG W., ZHOU J., FENG G., WEINDORF D.C., HU G., SHENG J. Characteristics of water erosion and conservation practice in arid regions of Central Asia: Xinjiang, China as an example. *International Soil and Water Conservation Research*. **3** (2), 98, **2015**.
- YIN J., YE M., YIN Z., XU S. A review of advances in urban flood risk analysis over China. *Stochastic Environmental Research and Risk Assessment*. **29** (3), 1064, **2015**.
- TAYYAB M., ZHANG J., HUSSAIN M., ULLAH S., LIU X., KHAN S.N., BAIG M.S., HASSAN W., AL-SHAIBAH B. GIS-Based Urban Flood Resilience Assessment Using Urban Flood Resilience Model: A Case Study of Peshawar City, Khyber Pakhtunkhwa, Pakistan. *Remote Sensing*. **13** (10), 1864, **2021**.
- ZHANG Q., GU X., SINGH V.P., SUN P., CHEN X., KONG D. Magnitude, frequency and timing of floods in the Tarim River basin, China: Changes, causes and implications. *Global and Planetary Change*. **139**, 44, **2016**.
- ORTON P.M., CONTICELLO F.R., CIOFFI F., HALL T.M., GEORGAS N., LALL U., MACMANUS K. Flood hazard assessment from storm tides, rain and sea level rise for a tidal river estuary. *Natural hazards*. **102** (2), 729, **2020**.
- DYER J.S. Remarks on the analytic hierarchy process. *Management science*. **36** (3), 249, **1990**.
- LIU J., XU Z., CHEN F., CHEN F., ZHANG L. Flood hazard mapping and assessment on the Angkor world heritage site, Cambodia. *Remote Sensing*. **11** (1), 98, **2019**.
- XIAO W., LV X., ZHAO Y., SUN H., LI J. Ecological resilience assessment of an arid coal mining area using index of entropy and linear weighted analysis: A case study of Shendong Coalfield, China. *Ecological Indicators*. **109**, 105843, **2020**.
- XIAO Y., YI S., TANG Z. A spatially explicit multi-criteria analysis method on solving spatial heterogeneity problems for flood hazard assessment. *Water Resources Management*. **32** (10), 3317, **2018**.
- YANG W., XU K., LIAN J., BIN L., MA C. Multiple flood vulnerability assessment approach based on fuzzy comprehensive evaluation method and coordinated development degree model. *Journal of environmental management*. **213**, 440, **2018**.
- LIU R., CHEN Y., WU J., GAO L., BARRETT D., XU T., YU J. Integrating entropy-based naïve Bayes and GIS for spatial evaluation of flood hazard. *Risk analysis*. **37** (4), 756, **2017**.
- METTERNICHT G., HURNI L., GOGU R. Remote sensing of landslides: An analysis of the potential contribution to geo-spatial systems for hazard assessment in mountainous environments. *Remote sensing of Environment*. **98** (2-3), 284, **2005**.
- BALOGUN A., QUAN S., PRADHAN B., DANO U., YEKEEN S. An improved flood susceptibility model for assessing the correlation of flood hazard and property prices using geospatial technology and fuzzy-ANP. *Journal of Environmental Informatics*. **37** (2), 107, **2020**.
- RAHMAN M., NINGSHENG C., ISLAM M.M., MAHMUD G.I., POURGHASEMI H.R., ALAM M., RAHIM M.A., BAIG M.A., BHATTACHARJEE A., DEWAN A. Development of flood hazard map and emergency relief operation system using hydrodynamic modeling and machine learning algorithm. *Journal of Cleaner Production*. **311**, 127594, **2021**.

21. WANG Z., LAI C., CHEN X., YANG B., ZHAO S., BAI X. Flood hazard risk assessment model based on random forest. *Journal of Hydrology*. **527**, 1140, **2015**.
22. SAHANI J., KUMAR P., DEBELE S., SPYROU C., LOUPIS M., ARAGÃO L., DI SABATINO S. Hydro-meteorological risk assessment methods and management by nature-based solutions. *Science of The Total Environment*. **696**, 133936, **2019**.
23. QUINN N., BATES P.D., NEAL J., SMITH A., WING O., SAMPSON C., HEFFERNAN J. The spatial dependence of flood hazard and risk in the United States. *Water Resources Research*. **55** (3), 1890, **2019**.
24. DI BALDASSARRE G., KEMERINK J.S., KOOY M., BRANDIMARTE L. Floods and societies: The spatial distribution of water-related disaster risk and its dynamics. *Wiley Interdisciplinary Reviews: Water*. **1**(2), 134, **2014**.
25. ZIARH G. F., ASADUZZAMAN M., DEWAN A., NASHWAN M. S., SHAHID S. Integration of catastrophe and entropy theories for flood risk mapping in peninsular Malaysia. *Journal of Flood Risk Management*. **14** (1), e12686, **2021**.
26. DEWAN A.M., KANKAM-YEBOAH K. Using synthetic aperture radar (SAR) data for mapping river water flooding in an urban landscape: a case study of Greater Dhaka, Bangladesh. *Journal of Japan Society of Hydrology and Water Resources* **19** (1), 50, **2006**.
27. CHEN F.H., CHEN J.H., HOLMES J., BOOMER I., AUSTIN P., GATES J.B., ZHANG J.W. Moisture changes over the last millennium in arid central Asia: a review, synthesis and comparison with monsoon region. *Quaternary Science Reviews*. **29** (7-8), 1061, **2010**.
28. MENG L., YANG X., ZHAO T., HE Q., MAMTIMIN A., WANG M., PAN H. Simulated regional transport structures and budgets of dust aerosols during a typical springtime dust storm in the Tarim Basin, Northwest China. *Atmospheric Research*. **238**, 104892, **2020**.
29. JIA J.P. *Statistics*. Tsinghua University Press. 68, **2004**.
30. KICHIGINA N. Geographical analysis of river flood hazard in Siberia. *International Journal of River Basin Management*. **18** (2), 260, 261, **2020**.
31. PAPA F., PRIGENT C., ROSSOW W. B. Monitoring flood and discharge variations in the large Siberian rivers from a multi-satellite technique. *Surveys in Geophysics*. **29** (4), 305, **2008**.
32. SAHARIA M., KIRSTETTER P.E., VERGARA H., GOURLEY J.J., HONG Y., GIROUD M. Mapping flash flood severity in the United States. *Journal of Hydrometeorology*. **18** (2), 402, **2017**.
33. VILLARINI G., SMITH J.A. Flood peak distributions for the eastern United States. *Water Resources Research*. **46** (6), W06504, **2010**.